International Journal of Environmental Engineering and Management
ISSN 2231-1319 Volume 8, Number 1 (2017), pp. 11-26

http://www.ripublication.com

El Niño & It's Effects on Climate Change

Gaurav Karhana*

New Delhi, India

Abstract

This paper emphasizes upon the El Niño and its effect on the global climate. The meaning of the term "El Niño" and how it has changed in time, so there is no universal single definition. The El Niño/southern oscillation (ENSO) phenomenon is the strongest natural inter annual climate fluctuation. ENSO originates in the tropical Pacific Ocean and has large effects on the ecology of the region, but it also influences the entire global climate system and affects the societies and the economics of many countries. One of the largest uncertainties concerns the relationship between ENSO characteristics and changes in the background climate state, whether natural or anthropogenic.To some extent, successful long-term climate prediction rests on the issue of whether the unusual severity of these events was a consequence of rising global temperatures or was simply representative of natural variability.ENS0 is now recognized as the single most important mode of the earth's year-to-year climatic variability. During the last decade, evidence has been accrued for the link between the Indian monsoon rainfall and ENSO.

Keywords:El Niño; Climate Change; Indian Monsoon; Gaurav Karhana.

1. INTRODUCTION

El Niño events, characterized by anomalous warming in the eastern equatorial Pacific Ocean, have global climatic teleconnections and are the most dominant feature of cyclic climate variability on sub decadal timescales. Understanding changes in the frequency or characteristics of El Niño events in a changing climate is therefore of broad scientific and socioeconomic interest. Recent studies show that the canonical El Niño has become less frequent and that a different kind of El Niño has become more

* Gaurav Karhana
*E-mail address:*gauravkh_bt2k16@dtu.ac.in

common during the late twentieth century, in which warm sea surface temperatures (SSTs) in the central Pacific are flanked on the east and west by cooler SSTs. This type of El Niño, termed the central Pacific El Niño (CP-El Niño; also termed the dateline El Niño, El Niño Modoki or warm pool El Niño), differs from the canonical eastern Pacific El Niño (EP-El Niño) in both the location of maximum SST anomalies and tropical–midlatitude teleconnections. Here we show changes in the ratio of CP-El Niño to EP-El Niño under projected global warming scenarios from the Coupled Model Intercomparison Project phase 3 multi-model data set. Using calculations based on historical El Niño indices, we find that projections of anthropogenic climate change are associated with an increased frequency of the CP-El Niño compared to the EP-El Niño. When restricted to the six climate models with the best representation of the twentieth-century ratio of CP-El Niño to EP-El Niño, the occurrence ratio of CP-El Niño/EP-El Niño is projected to increase as much as five times under global warming. The change is related to a flattening of the thermocline in the equatorial Pacific.

ENSO & tropical pacific climate during last millennium

The term "El Niño" originally applied to an annual weak warm ocean current that ran southward along the coast of Peru and Ecuador about Christmas Time (hence Niño, Spanish for "the boy Christ-child") and only subsequently became associated with the unusually large warmings that occur every few years and change the local and regional ecology. The coastal warming, however, is often associated with a much more extensive anomalous ocean warming to the International Date Line, and it is this Pacific basin wide phenomenon that forms the link with the anomalous global climate patterns. The atmospheric component tied to El Niño is termed the "Southern Oscillation." Scientists often call the phenomenon where the atmosphere and ocean collaborate together ENSO, short for El Niño–Southern Oscillation. El Niño then corresponds to the warm phase of ENSO. The opposite "La Niña" ("the girl" in Spanish) phase consists of a basin wide cooling of the tropical Pacific and thus the cold phase of ENSO. However, for the public, the term for the whole phenomenon is "El Niño." Accordingly, it has been very difficult to define El Niño or an El Niño event. The term has changed meaning: some scientists confine the term to the coastal phenomenon, while others use it to refer to the basin wide phenomenon, and the public does not draw any distinction. There is considerable confusion, and past attempts to define El Niño have not led to general acceptance. Clearly, the term El Niño covers a diverse range of phenomena. Earlier, Glantz and Thompson (1981, 3–5) pointed out the numerous meanings of El Niño and a general review of the terminology confusion was given by Aceituno (1992). Glantz (1996) has formally put forward a definition of El Niño as it should appear in a dictionary:

El Niño \ 'el ne- ' nyo- noun [Spanish] \ 1: The Christ Child 2: the name given by Peruvian sailors to a seasonal, warm southward-moving current along the Peruvian coast 3: name given to the occasional return of unusually warm water in the normally cold water [upwelling] region along the Peruvian coast, disrupting local fish and bird populations 4: name given to a Pacific basin-wide increase in both sea surface temperatures in the central and/or eastern equatorial Pacific Ocean and in sea level atmospheric pressure in the western Pacific (Southern Oscillation) 5: used interchangeably with ENSO (El Niño–Southern Oscillation) which describes the basin wide changes in air–sea interaction in the equatorial Pacific region 6: ENSO warm event synonym warm event antonym La Niña \ [Spanish] \ the young girl; cold event; ENSO cold event; non-El Niño year; anti-El Niño or anti-ENSO (pejorative); El Viejo \ 'el vya- ho- \ noun [Spanish] \ the old man.

This definition reflects the multitude of uses for the term but is not quantitative. There have been several attempts made to make quantitative definitions, although always by choosing just one of the myriad of possibilities and therefore falling short for general acceptance. Quinn et al. (1978) provided a listing of El Niño events and a measure of event intensity on a scale of 1 to 4 (strong, moderate, weak, and very weak) beginning in 1726. The measures used to define the El Niño and its intensity were primarily based on phenomena along the coast of South America and were often qualitative. In the early 1980s, a Scientific Committee for Ocean Research working group, SCOR WG 55, was set up to define El Niño (SCOR 1983) and came up with the following:

El Niño is the appearance of anomalously warm water along the coast of Ecuador and Peru as far south as Lima (12°S). This means a normalized sea surface temperature (SST) anomaly exceeding one standard deviation for at least four (4) consecutive months. This normalized SST anomaly should occur at least at three (3) of five (5) Peruvian coastal stations

Tropical pacific climate variability

We generate multi-century, monthly resolved records of tropical Pacific climate variability over the last millennium by splicing together overlapping fossil-coral records from the central tropical Pacific. These precisely dated, well-reproduced records allow us to characterize the range of natural variability in the tropical Pacific climate system with unprecedented fidelity and detail. Collectively, the records document a wide range of ENSO characteristics, along with substantial decadal-scale variability and subtler centennial-scale fluctuations in tropical Pacific climate over the last millennium. We analyse the variability contained in monthly resolved coral δ18O records from five intervals of the last millennium: AD 928–961, 1149–1220, 1317–1464, 1635–1703 and 1886–1998 (Fig. 5). The tenth- and twelfth-century sequences represent single fossil-coral δ18O records, the fourteenth–fifteenth- and the

seventeenth-century sequences are spliced fossil-coral δ18O records, and the twentieth century sequence is the modern coral δ18O record. Time-series analyses of the fossil-coral records reveal a range of ENSO frequencies and amplitudes exceeding that exhibited in the twentieth-century coral (Fig. 6a and b). For example, some seventeenth-century El Niño events rival the 1997 El Niño event in severity. ENSO activity in the seventeenth-century sequence is not only stronger (in terms of variance), but more frequent than ENSO activity in the late twentieth century. This conclusion holds for a variety of time-series analysis techniques, including spectral analysis and a range of different band pass filters. On the other extreme, there are 30-yr intervals during both the twelfth and fourteenth centuries when ENSO activity is greatly reduced relative to twentieth-century observations. Taken together, the fossil corals portray a highly variable ENSO over the last millennium whose amplitude and frequency changed markedly, in some cases over the course of a decade. The fossil-coral data allow for a critical assessment of several theories that have been proposed to explain ENSO variability. First, the data test the suggestion that changes in the mean state, whether through natural decadal-scale variability or greenhouse warming, may alter ENSO characteristics. The relationship between ENSO variance and mean coral δ18O is weak (R ¼ 0.43), mostly because ENSO variance changed significantly while mean coral δ18O remained relatively stable during the fourteenth–fifteenth centuries (Fig. 6a and c, and Supplementary Fig. S2). Overall, the corals resolve a broad range of ENSO variances that cannot be explained by changes in the mean state. An alternative explanation for the observed irregularity of ENSO is that noise in the climate system, most likely of atmospheric origin, interferes with the recharge oscillator that is thought to set ENSO's periodicity. If random noise is the dominant source of ENSO's variability, then ENSO indices should be stationary—that is, the statistics of the time series (its spectral properties and variance) should not change appreciably through time. However, two of the fossil-coral sequences—the records from the twelfth and the fourteenth–fifteenth centuries—exhibit significant changes in ENSO behaviour from decade to decade (Fig. 6a). A definitive test for non-stationary behaviour requires longer records than those available at present, but the coral records produced thus far suggest that large fluctuations in ENSO variance are fundamental to the physics of the phenomenon. In fact, the behaviourexhibited by the coral records is reminiscent of ENSO 'regime changes' that occur in a variety of ENSO models whose variability is partially a product of chaos. The potential for regime-like changes in ENSO characteristics carries important implications for future climate changes under continued greenhouse forcing, because it allows for a nonlinear response of the global climate system to linear forcing. Apart from ENSO variability, the Palmyra corals also resolve substantial decadal-scale variability that acts on a broad range of timescales from 8 to 30 yr. Power spectra of the records show no sign of a preferred periodicity for this low-frequency variability, which approaches a red noise continuum in the 150-year-long sequence (not shown). However, it is clear from a

comparison of Fig. 6a and c that decadal-scale variability is distinguishable from the decadal modulation of ENSO. This observation implies that the dynamics that underlie decadal-scale variability must be distinct from those of ENSO. Given that coral δ18O is a mixed SST and sea surface salinity signal, it is difficult to translate mean coral δ18O into firm estimates of century-scale SST variability. However, if we assume that warmer SST is tightly coupled to anomalous convection in the central tropical Pacific on centennial timescales, as it is on interannual timescales, then the Palmyra corals provide unique constraints on the evolution of mean climate in the central tropical Pacific over the last millennium. Evidence for a tight SST–rainfall coupling on timescales longer than ENSO comes from the late-twentieth-century trend in coral δ18O. Recent estimates of central tropical Pacific warming since the 1970s are 0.8 8C19, which would correspond to a, 0.14‰ decrease in coral δ18O, using the SST/δ18O calibration from Fig. 2. The actual change in the coral δ18O over this time period is about 20.30‰, a roughly twofold amplification that must be ascribed, at least in part; to regional-scale freshening that accompanied central tropical Pacific warming. If twentieth-century SST–rainfall relationships apply throughout the last millennium, then the Palmyra fossil corals should be sensitive recorders of mean climate change in the central tropical Pacific. That said, mean coral δ18O values for the twelfth, fourteenth– fifteenth, seventeenth and early twentieth centuries vary within a relatively narrow 0.14‰ range (or 0.6 8C, if scaled to temperature alone). The only significant departures in mean coral δ18O occur in the tenth century and late-twentieth-century sequences. It seems probable that the tenth century witnessed the coolest and/or driest conditions in the central tropical Pacific of the last 1,100 years, although this conclusion must be verified by additional tenth century coral records. The late twentieth century, the period covered by dense instrumental climate data, represents the warmest, wettest interval of the last millennium.

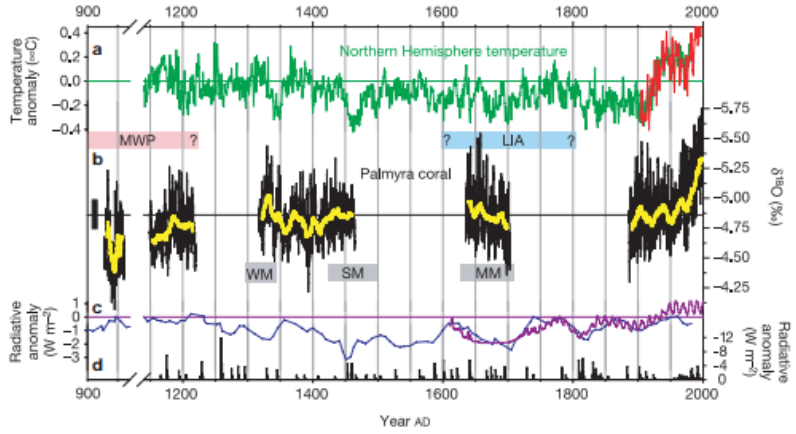

Figure 5 Comparison of proxy climate records and external forcing during the last millennium. **a**, The MBH Northern Hemisphere temperature reconstruction[34] (green) plotted with the Northern Hemisphere instrumental temperature record of ref. 48 (red). The green horizontal line denotes the mean of the MBH record for the period AD 1886–1975. **b**, The monthly resolved Palmyra coral $\delta^{18}O$ records (thin black line), shown with a 10-yr running average (thick yellow line). The black horizontal line represents the average of the Palmyra modern coral $\delta^{18}O$ for the period AD 1886–1975. The black vertical bar represents the $\pm 1\sigma$ error in mean coral $\delta^{18}O$ for single fossil corals (this error applies only to tenth- and twelfth-century sequences). The dating error is ± 10 yr for the tenth- and twelfth-century sequences, ± 5 yr for the fourteenth–fifteenth- and seventeenth-century sequences, and $\pm < 0.5$ yr for the twentieth-century sequence. **c**, Reconstruction of solar irradiance anomalies based on historical sunspot records (anomalies calculated with respect to the AD 1886–1975 mean)[49] (purple) plotted with ^{10}Be anomalies (a proxy for solar activity)[50] (blue), plotted as a 3-point running mean and scaled to the solar irradiance anomalies. **d**, Radiative forcing associated with volcanic eruptions recorded in ice cores (black)[35]. The approximate timing and duration of the 'Little Ice Age' (LIA), the 'Medieval Warm Period' (MWP), and solar activity minima—the Maunder minimum (MM), the Spörer minimum (SP), and the Wolfe minimum (WM)—are marked by horizontal bars.

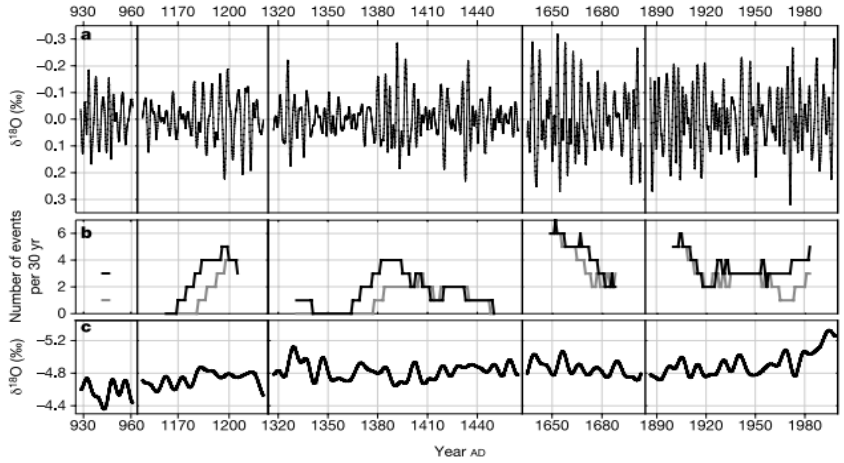

Figure 6 ENSO and lower-frequency components of the Palmyra coral $\delta^{18}O$ records. **a**, ENSO variability isolated by applying a 2–7-yr bandpass filter to the deseasoned monthly coral $\delta^{18}O$ anomaly data, plotted contiguously. **b**, An index of ENSO activity, defined as the number of El Niño (black) and La Niña (grey) events in a sliding 30-yr window. An El Niño (La Niña) event is defined by annual-mean $\delta^{18}O$ anomalies (computed from the 2–7-yr bandpass filter series, centred on January) that are less than (greater than) −0.11‰ (+0.11‰). This threshold corresponds to one standard deviation of the modern coral's 2–7-yr bandpassed record, and is roughly equivalent to NIÑO3.4 SST anomalies of 0.6 °C, according to the calibration presented in Fig. 2. **c**, Lower-frequency climate variability isolated by applying an 8-yr lowpass filter to the coral $\delta^{18}O$ data.

ENSO & Winter precipitation extremes over India

In India, large agricultural economy increases the importance of any changes in precipitation distribution. Variability of winter precipitation over India is known to be associated with temperature variability over equatorial Indian Ocean (Kripalani and Kumar P, 2004) as well as over the Pacific (Kumar P et al., 2007). Extreme rainfall results in flash floods and crop damage that have a major impact on society, the economy and the environment. Inspired by Goswami's study (2006), one of the main

purpose of this study is to identify any possible long-term trend in daily extreme winter precipitation over South-east Indian domain. We also attempt to study the changes in frequency and intensity of extreme winter precipitation events over India and their modulation by temperatures over equatorial Pacific.

A number of studies have shown that there is a strong positive co-relationship between the SSTs overNiño3.4 region and the winter-monsoon rainfall (Oct-Nov-Dec) over the south-eastern tip of the Indian land mass. Normally this region gets rainfall in October–December period due to weather systems like tropical cyclones, depressions, North–south trough activity and coastal convergence. During El Niño years, the wind flow at lower levels is predominantly easterlies with strong westerlies aloft. This situation generates a vertical wind shear in this region, which is the inhibitive factor for cyclone genesis, hence strong easterly waves are associated with excessive rainfall over the region. Singh and Chattopadhyaya (1998) have shown that the seasonal spring (March–April–May) southern oscillation index is positively correlated with rainfall over the southeast Indian region of Tamil Nadu, coastal Andhra Pradesh and Rayalseema. The correlation between monthlyNiño3.4 SSTs and the frequencies of extremes are shown in Figure 6. The top panel shows correlation with frequencies based on percentiles. These correlations are based on the 30- year period 1971–2000. The frequency for the 65th percentile shows maximum correlation coefficient (CC) with July SSTs (CC = 0.54) while the 75th percentile frequency has maximum relationship (CC = 0.55) with May SSTs and the 85th percentile frequency with April SSTs (CC = 0.52). The relationship assumes significance from July–August of the previous year; it goes on strengthening as time progresses and reaches its maximum, thus, 5 (April), 4 (May) and 3 (June) months before the winter monsoon (October–December) sets in. Similarly, for fixed thresholds of 30, 20 and 10 mm, theNiño3.4 SSTs, in the month of May before the onset of winter monsoon are strongly correlated (CC = 0.52, 0.55 and 0.52 respectively) with respective frequencies. The correlations are significant at 1% level (>0.478) The frequencies obtained by using different thresholds as suggested by Goswami et al. (2006) are also correlated withNiño3.4 SSTs and they give very encouraging results. The frequencies of moderate events are strongly related withNiño3.4 SSTs, the CC is of the order of 0.5 in the month of April before winter monsoon. Whereas, the heavy rainfall events (30–50 mm) are weakly correlated with Niño.3.4 SSTs. The number of days with very high precipitation amounts (more than 50 mm) show a strong relationship in previous April (CC = 0.59) implying that the number of very high rainfall days can be very well predicted 5 months in advance with the help ofNiño3.4 SSTs. The correlation analysis shows that the prediction of number of extreme rainfall events in winter season can be made with reasonably good skill fromNiño3.4 SSTs as early as April–May–June. The correlations between the intensity of 1-day and 5- day maximum precipitation with monthlyNiño3.4 SSTs are shown in Figure 7. The 1-day maximum precipitation has significant relationship with preceding April SSTs, then the

relationship goes on strengthening and is maximum of the order of 0.45 in the month June–July, two months before the winter monsoon starts. The correlation of 0.45 is significant at 5% level for the sample of 30. Also 5-day maximum precipitation has the CC of order of 0.38, with preceding January SSTs, significant at 5% level. 5-day precipitation intensity is not as strongly related withNiño3.4 SSTs, as 1-day precipitation intensity. HenceNiño3.4 SSTs in the month of June can be used to get some idea of 1-day maximum precipitation in the coming winter monsoon. The spell lengths of continuous dry/wet days do not show good relationship withNiño3.4 SSTs (hence figure is not presented). Spell lengths of continuous dry (wet) days are negatively (positively) correlated withNiño3.4 SSTs since previous June–July, which is obvious since winter precipitation is known to be positively related withNiño3.4 SSTs and the good winter precipitation is characterized by more number of long wet spells.

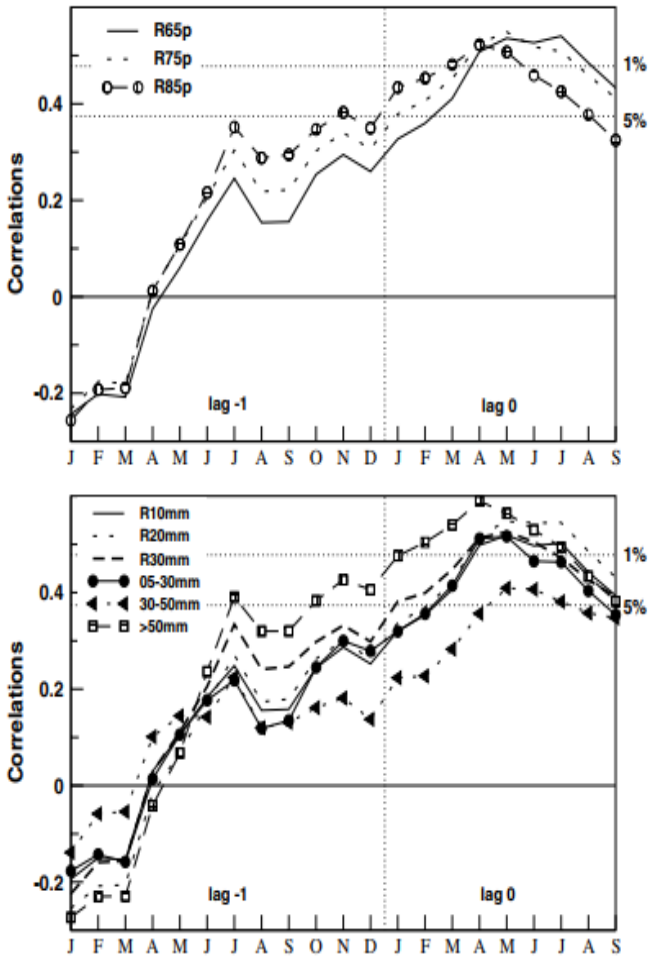

Figure 6. Correlations of NINO3.4 SSTs with frequency of extremes based on percentiles (top panel) and fixed thresholds (botton panel) based on 1971–2000. The dotted horizontal lines are significant correlation coefficients at the 1and 5% level.

Climatic Impact of EN/LN on the Indian monsoon

The most exciting research on the interannual scale in the tropics has undoubtedly been on the links between the monsoons and the ENSO phenomenon (Glantz et al. 1991; Webster and Yang 1992). Sikka (1980) showed that El Niño and monsoon failures over India are related on a year-to-year basis, with a failure of the monsoon in the majority of the El Niño cases. Rasmusson and Carpenter's (1983) detailed analysis based on better indices for El Niño suggested that the relationship between El Niño and monsoon failures is even stronger than that suggested by Sikka's study. A review of the work done on the r61e of ENSO in monsoon variability is given in Krishna Kumar el al. (1995). In summary, during the ENSO warm (cold) extremes the majority of the episodes induce below (above) normal rainfall. Hence, besides the internal epochal variability, drought flood conditions can occur due to an external forcing such as El Niño La Niña. During the period 1871-1990, there were 27 occurrences of El Niño events (Rasmusson and Carpenter 1983; Climate Analysis Center 1995) and 23 occurrences of La Niña events (Van Loon and Shea 1985). These episodes are tabulated in Table 1 along with the standardized NSMR associated with each of these episodes. Although the period 1930-63 (1895-1930) was an epoch of above (below) normal rainfall, the El Niño s (La Niña s) of 1941 and 1951 (1908 and 1916) caused below (above) normal rainfall, suggesting that an external forcing can break the rhythm of the epochal behavior. Given that the El Niño La Niña episodes do have an impact during the opposite phase of the epochal variability, let us now examine what happens if the El Niño La Niña events and the epochs are in phase, i.e. the impact of El Niño(La Niña) during the below (above) normal rainfall epochs. Over the past 120 years (1871-1990) there have been 11 occurrences of very strong El Niño episodes (1877, 1884, 1891, 1899, 1911, 1918, 1925, 1941, 1957, 1972, 1982, see Quinn et ul. (1987)). the worst drought situations over India were recorded during 1877, 1899, 1918 and 1972. Interestingly, all these years fall during the below normal phase of the epochal variability. However, the strong El Niño s of 1884, 1891, 1941 and 1957 did not result in extreme drought situations over India, probably because these episodes are during the above normal phase of the epochal variability. The impact of the 1911 and 1982 El Niño s during the below normal rainfall epochs was substantial, while that of the 1925 El Niño was not. Hence, when the internal epochal variability and the external forcing (El Niño) are in phase, an extreme situation can occur. Thus the impact of El Niño on the AISMR is more severe during the below normal epochs than during the above normal epochs. The average standardized AISMK for the 16 (9) El Niño cases in the below (above) normal rainfall epochs is -1.2 (-0.4), while for the 8 (15) La Niña cases in the above (below) normal rainfall epochs it is +0.8 (+0.5) - see Table 1. The differences between the means for the El Niño cases are significant at the 5 per cent confidence level; however, the differences between the means for the La Niña cases are not significant at this level. If we exclude the two El Niño cases during 1914 and 1976 (there was rather chaotic

smaller-amplitude variability around these years, see Fig. l(b)), then the average standardized AISMR for 14 El Niño cases in the below normal epochs is -1.5. Then the differences between the means for the El Niño cases are significant even at the 1 per cent confidence level. It appears that the phase locking between ENSO cold extremes and the above normal epochal variability is not as striking as between the warm extremes and the below normal phase. Hence the major extreme events of rainfall (severe droughts floods) in particular dry periods are due to the phase locking between the internal epochal variability and the external forcing of El Niño. Thus the impact of El Niño on the Indian monsoon rainfall is not the same during the epochs of above and below normal rainfall.

Table 1. Years of El Niño and La Niña events

El Niño

B (16)	1877 -3.0	1896 -0.3	1899 -2.7	1902 -0.7	1905 -1.6	1911 -1.4	1914 +0.5	1918 -2.4	1923 -0.3	1925 -0.6	1965 -1.7
	1969 -0.3	1972 -2.4	1976 +0.1	1982 -1.4	1987 -1.9						
A (9)	1884 +1.0	1887 +0.6	1891 -0.7	1932 -0.6	1939 -0.7	1941 -1.5	1951 -1.3	1953 +0.8	1957 -0.8		
T (2)	1880 -0.4	1930 -0.6									

La Niña

B (15)	1898 +0.4	1903 +0.1	1906 +0.4	1908 +0.5	1916 +1.2	1920 -1.6	1924 +0.1	1964 +0.8	1966 -1.3	1970 +1.0	1973 +0.7
	1975 +1.3	1978 +0.7	1983 +1.2	1988 +1.3							
A (8)	1886 +0.3	1889 +0.9	1892 +1.7	1931 +0.3	1938 +0.7	1942 +1.3	1949 +0.6	1954 +0.4			

In many seasonal forecast tools, Indian monsoon rains are predicted to vary in direct proportion to the strength of the El Niño Southern Oscillation (ENSO) phenomenon in the tropical Pacific (5–7), measured, for example, by the standardized NIÑO3 index (8). Indeed, years with moderate to extreme cold states (NIÑO3 index G –1), have had abundant monsoon rains without exception. On the other hand, years of moderate to extreme warm states have not been reliably dry. As seen in Fig. 1, the six leading droughts (8) since 1871 have occurred in tandem with a standardized NIÑO3 index exceeding þ1, but the presence of El Niños has not guaranteed drought. No simple association describes the relation between the Indian monsoon and NIÑO3 SSTs when moderate to strong El Niño conditions exist; almost a full range of monsoon rains have accompanied SST warmings. For example, 1997 was the century's

strongest El Niño, although no drought occurred, whereas the moderate El Niño of 2002 was accompanied by one of the worst Indian droughts of the past century (4). Such ambiguity undermines the utility of monsoon predictions for mitigation of droughts societal impacts. Two hypotheses have been proposed to explain this ambiguity in the El Niño–Indian monsoon relationship. One is that chaotic variability in rainfall on intraseasonal time scales masks the remote effect of El Niño. Accordingly, the failure (abundance) of monsoon rains during 2002 (1997) would be viewed as the accidental behavior of an inherently noisy monsoon system, and the poor forecasts for these particular cases were the consequence of an only marginally predictable system. The other is that the Indian monsoon is highly sensitive to the details of tropical east Pacific sea surface warming. It is widely believed that El Niños impact on the Indian monsoon is through the east-west displacement of the ascending and descending branches of the Walker circulation that link Indo-Pacific climates (9, 10). Unusually warm waters during El Niño cause an increased ascent associated with increased rainfall. Mass continuity requires increased descent broadly over Southeast Asia, suppressing monsoon rains. The hypothesis we explore is that the strength and position of these branches vary coherently with the details of El Niño warming. We begin by examining the 23 strong El Niño years for atmosphere and ocean conditions that distinguish the 10 Indian monsoon droughts from the 13 drought-free years. Figure 2A illustrates their contrasting sea surface temperatures (SSTs). The most notable difference in the tropical Pacific SSTs is the greater central Pacific warming during failed Indian monsoon years (Fig. 2A). These analyses suggest that India is more prone to drought when the ocean warming signature of El Niño extends westward. Figure 2B displays the difference in tropical rainfall for the drought versus drought-free El Niño years. Although rainfall data are based on a smaller sample of cases for which satellite rainfall estimates are available, a physical consistency with the underlying SST anomalies in Fig. 2A is apparent. Increased rainfall occurs over the enhanced warmth of central Pacific Ocean waters, and the satellite estimates confirm dryness over India, the Indian Ocean, and other portions of Southeast Asia, indicating a wide reach to the drought signal. These rainfall anomalies form a dynamical couple that is linked by an Indo-Pacific anomalous Walker circulation, as seen in the velocity potential (8) at 200 hPa (Fig. 2B, contours). The composite anomaly differences highlighted by shading in Fig. 2, A and B, are statistically significant (8) and are physically consistent with the expected rainfall-SST relationship. This is further seen by the separability of the probability density functions (PDFs) (8) of rainfall for drought versus drought-free years (Fig. 2C). Although this empirical analysis does not establish causal linkages, it does suggest that the two B flavors [of El Niño (11) result in significantly different responses in the Indian monsoon. The SST patterns of these two flavors can be described by a linear combination of the two leading, preferred patterns of tropical Pacific SST variability of the past half century (8), shown in Fig. 3. The first leading pattern (Fig. 3A)

represents the overall strength of the ENSO events, and its associated temporal pattern is highly correlated with fluctuations in the NIÑO3 index (Fig. 3C). The second pattern (Fig. 3B) has polarity of opposite sign between the tropical Central and Eastern Pacific, and its temporal pattern is highly correlated with fluctuations of an index that measures the SST gradient across the Pacific basin (8) (Fig. 3D). We note in particular that the second leading pattern closely resembles the SST difference between severe drought and drought-free monsoon years (Fig. 2A, shaded). General circulation model (GCM) experiments (8), forced with SST patterns resulting from linear combinations of the first two leading patterns of tropical Pacific SST variability, are used to test the hypothesis that B westward shifted [Pacific Ocean warm events drive more intense sinking over the Indian region, initiating severe drought. Using National Center for Atmospheric Research–Community Climate Model Version 3, we performed four ensemble sets of experiments: (i) a 150-year control run of the GCM forced by monthly evolving global climatological mean SST; (ii) a fixed SST pattern resulting from the addition of the first two leading tropical Pacific SST patterns superimposed on the monthly evolving climatological SSTs globally; (iii) same as (ii), but subtracting the second leading tropical Pacific SST pattern from the first; and (iv) an SST pattern corresponding to the first leading pattern (i.e., Fig. 3A) alone. The model experiments for (ii), (iii), and (iv) were performed for a range of imposed SST warmth from 0 to þ3 standard deviations (SD), with results available at an interval of 0.2 SD. We analyzed 10 simulations with different initial atmospheric conditions for each of these incremental warmings.

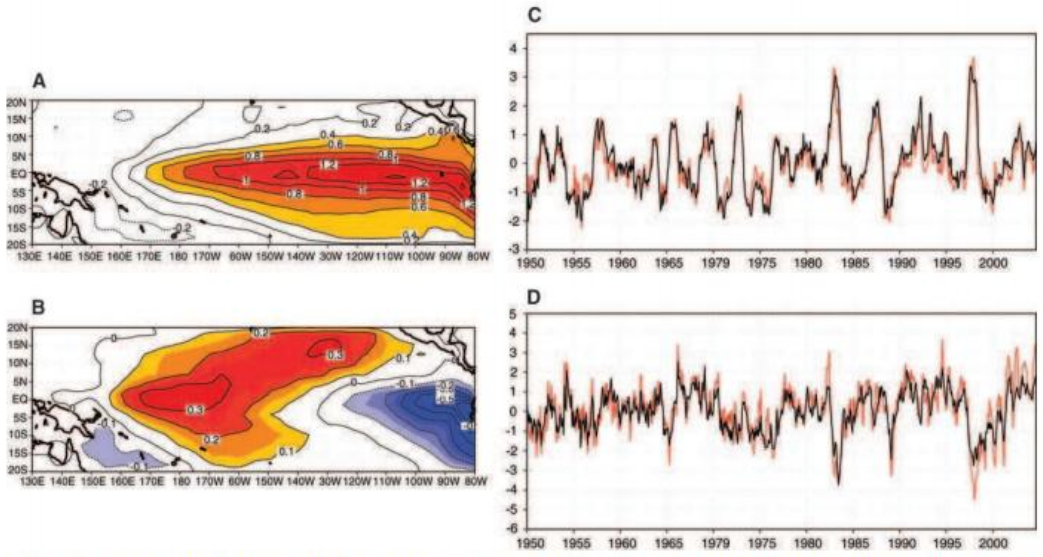

Fig. 3. (**A**) The first leading pattern of the tropical Pacific SST variability. (**B**) Same as (A) but for the second leading pattern. (**C**) The first leading temporal pattern (black line) overlaid with the monthly NINO3 index (red line). (**D**) The second leading temporal pattern (black line) overlaid with the trans-Niño index (TNI) (red line).

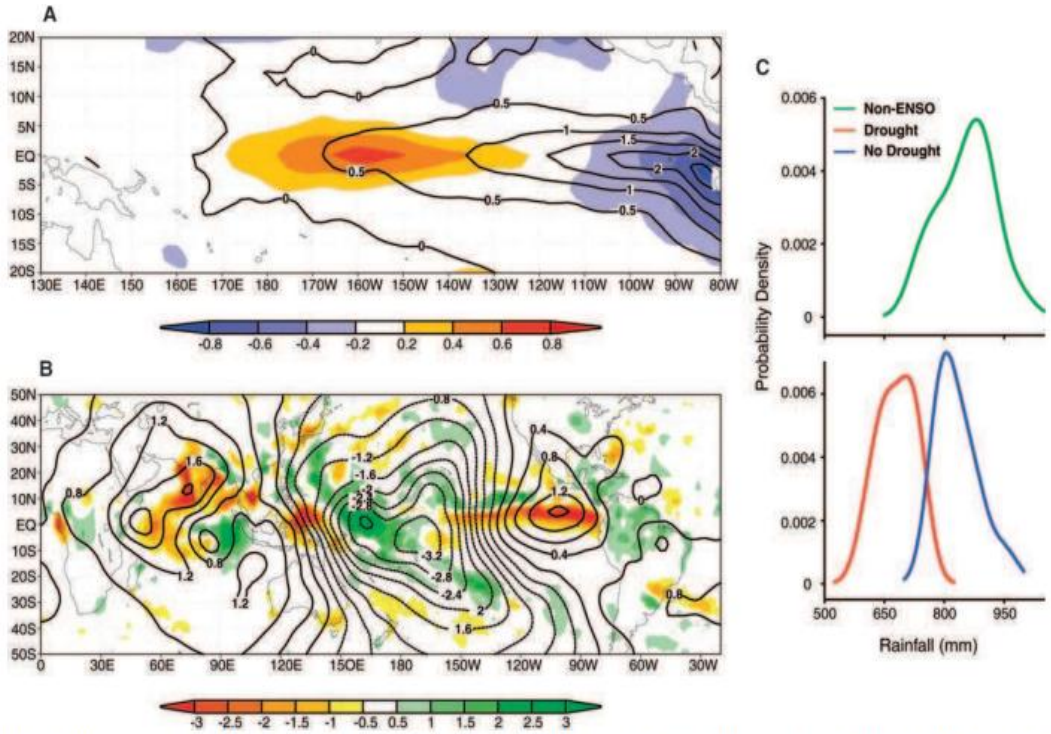

Fig. 2. **(A)** Composite SST difference pattern between severe drought (shaded) and drought-free El Niño years. Composite SST anomaly patterns of drought-free years are shown as contours. **(B)** Composite difference pattern between severe drought and drought-free years of velocity potential (contours) and rainfall (shaded). **(C)** PDF of all-India summer monsoon rainfall from severe-drought (red curve) and drought-free (blue curve) years associated with El Nino occurrence and from the non-ENSO years (green curve). SST and velocity potential composite differences are based on 1950 to 2004, rainfall composites are based on 1979 to 2004, and PDFs are based on 1873 to 2004.

SUMMARY

It is hoped that the above provides a quantification of ENSO events in several ways, including when they have occurred, their duration. A listing of the duration of the El Niño and La Niña events after 1950 is provided. Nevertheless, these measures are not unique and alternative criteria can be used. In particular, different criteria might be used if the interest is the coast of South America, where the term El Niño originated.The El Niño-southern oscillation has been shown to be strongly related with variations in frequencies of extreme precipitation in winter season over India. The number of extreme events increases in the year after the onset of El Niño events. Strong correlations exist between the frequency and intensity of extreme precipitation events and NIÑO 3.4 SSTS 4–6 months in advance but no relationship exists for spell lengths of continuous wet/dry days and an index of ENSO. Very heavy rainfall events possess very strong relationship with April SSTs over NIÑO3.4 region hence it is possible to predict very heavy rainfall events well in advance.Through the analysis of the short-term fluctuations of seasonal rainfall time-series, it was found that there are epochs of above and below normal rainfall. This epochal behavior could be broken by a strong external forcing such as El Niño. The major extreme events of rainfall (severe floods/droughts) are due to the phase-locking between the epochal variability

and the external forcing; i.e. the impact of El Niño (La Niña) on the AISMR is more severe during the below (above) normal epochs. The epochal behavior is not forced by the frequencies of the El Niño/La Niña events. It should be noted that in some years a monsoon drought occurs without the occurrence of an El Niño event, the worst being during 1979 (standardized AISMR -1.7). Other factors are also believed to be important for the inter annual behavior of the AISMR. A recent study by Kripalani et al. (1996) suggests that the Eurasian snow mass is better related to the Indian monsoon than the snow-cover

REFERENCES

[1] El Niño in a changing climate Sang-Wook Yeh , Jong-Seong Kug , Boris Dewitte , Min-Ho Kwon , Ben P. Kirtman & Fei-Fei Jin

[2] Unraveling the Mystery of Indian Monsoon Failure During El Niño K. Krishna Kumar, Balaji Rajagopalan ,Martin Hoerling,Gary Bates ,Mark Cane

[3] The Definition of El Niño Kevin E. Trenberth National Center for Atmospheric Research,* Boulder, Colorado

[4] El Niño/Southern Oscillation and tropical Pacific climate during the last millennium Kim M. Cobb*†, Christopher D. Charles*, Hai Cheng‡ & R. Lawrence Edwards‡ * Scripps Institution of Oceanography, University of California-San Diego, La Jolla, California 92093, USA ‡ Minnesota Isotope Laboratory, Department of Geology and Geophysics, University of Minnesota, Minneapolis, Minnesota 55455, USA

[5] Climatic impact of El Niño/La Niña on the Indian monsoon: A new perspective R. H. Kripalani and Ashwini Kulkarni Indian Institute of Tropical Meteorology, Pune, India Contact Information

[6] The El Niño-Southern Oscillation and winter precipitation extremes over India J. V. Revadekar* and Ashwini Kulkarni Indian Institute of Tropical Meteorology, Dr. Homi Bhabha, Road, Pashan, Pune-411008, India

[7] Bhalme, H. N. and Jadhav, S. K. (1984) The double (Hale) sunspot cycle and floods and droughts in India. Weah, 39, pp. 112-116

[8] Materials and methods are available as supporting material on Science Online.

[9] J. Shukla, in Monsoons, J. S. Fein, P. L. Stephens, Eds. (Wiley, New York, 1987).

[10] C. F. Ropelewski, M. S. Halpert, Mon. Weather Rev. 115, 1606 (1987).

[11] K. Trenberth, Proc. 18th Ann. Clim. Diagnost. Workshop, Boulder, CO, 50 (1993).

[12] N. H. Saji, B. N. Goswamy, P. N. Vinayachandran, T. Yamagata, Nature 401, 360 (1999).

[13] K. Krishna Kumar, K. Rupa Kumar, R. G. Ashrit, N. R. Deshpande, J. W. Hansen, Int. J. Climatol. 24, 1375 (2004).

[14] S. G. Philander, Our Affair with El Nin˜ o (Princeton Univ. Press, Princeton, NJ, 2004).

[15] S. Gadgil et al., Curr. Sci. 83, 394 (2002).

[16] S. Gadgil, M. Rajeevan, R. Nanjundiah, Curr. Sci. 88, 1389 (2005).

[17] S. Hastenrath, Climate Dynamics of the Tropics (Kluwer Academic Publishers, Dordrecht, Netherlands, 1991).

[18] K. Krishna Kumar, M. K. Soman, K. Rupa Kumar, Weather 50, 449 (1995).

[19] McPhaden, M. J. & Zhang, D. X. Slowdown of the meridional overturning circulation in the upper Pacific Ocean. Nature 415, 603–608 (2002).

[20] Cole, J. E., Fairbanks, R. G. & Shen, G. T. Recent variability in the Southern Oscillation—isotopic results from a Tarawa Atoll coral. Science 260, 1790–1793 (1993).

[21] Evans, M. N., Fairbanks, R. G. & Rubenstone, J. L. The thermal oceanographic signal of El Nin˜o reconstructed from a Kiritimati Island coral. J. Geophys. Res. C 104, 13409–13421 (1999).

[22] Urban, F. E., Cole, J. E. & Overpeck, J. T. Influence of mean climate change on climate variability from a 155-year tropical Pacific coral record. Nature 407, 989–993 (2000).

[23] Cobb, K. M., Charles, C. D. & Hunter, D. E. A central tropical Pacific coral demonstrates Pacific, Indian, and Atlantic decadal climate connections. Geophys. Res. Lett. 28, 2209–2212 (2001).

[24] McCulloch, M. et al. High-resolution windows into early Holocene climate: Sr/Ca coral records from the Huon Peninsula. Earth Planet. Sci. Lett. 138, 169–178 (1996).

[25] Tudhope, A. W. et al. Variability in the El Nin˜o–Southern Oscillation through a glacial-interglacial cycle. Science 291, 1511–1517 (2001).

[26] Hughen, K. A., Schrag, D. P., Jacobsen, S. B. & Hantoro, W. El Nin˜o during the last interglacial period recorded by a fossil coral from Indonesia. Geophys. Res. Lett. 26, 3129–3132 (1999).

[27] Scoffin, T. P. The geological effects of hurricanes on coral reefs and the interpretation of storm deposits. Coral Reefs 12, 203–221 (1993).

[28] Cobb, K. M., Charles, C. D., Cheng, H., Kastner, M. & Edwards, R. L. U/Th-dating living and young fossil corals from the central tropical Pacific. Earth Planet. Sci. Lett. 210, 91–103 (2003).